Dynamic Control Strategy of a Biped Inspired from Human Walking

Hayssam Serhan, Patrick Henaff, Chaiban G. Nasr, Fethi Ben Ouezdou

Dynamic Control Strategy of a Biped Inspired from Human Walking

H. Serhan, P. Hénaff (IEEE Member), C. Nasr (SM IEEE), F. Ouezdou (IEEE Member)

Abstract— **In this paper, we show that a biped robot can walk dynamically using a simple control technique inspired from human locomotion. We introduce four critical angles that affect robot speed and step length. Our control approach consists in tuning the PID parameters of each joint in each walking phase for introducing active compliance and then to increase stability of the walk. We validated the control approach to a dynamic simulation of our 14DOF biped called ROBIAN. A comparison with human walking is presented and discussed. We prove that we can maintain robot stability and walk cycle's repetition without referencing a predefined trajectory or detecting the center of pressure. Results show that the walk of the biped is very similar to human one. A power consumption analysis confirms that our approach could be implemented on the real robot ROBIAN.**

I. Introduction

Biorobotics research seeks to develop new robotic technologies modeled after the performance of human and animal neuromuscular systems. These techniques lead to complex control strategies. The implementation of such control approaches in biped walking robot did not enhance the robot locomotion to mimic the human one. In addition, those techniques required many mechanical customization or simplifications. Those customizations contributed to a non-human model. However, observation of human walking let one assumes that this walk is seemingly simple. Walking inspiration from human being could be done by trying to mimic natural human locomotion on many different ways. The more common methods are:

- Biologically inspired control approaches using neural oscillators as a central pattern generator (CPG) and reflexive control [1][2][3].
- Passive dynamic walking approach and its extension to active feedback [4]-[7], [9]-[16].
- Pragmatic rules for real-time control [8].
- Tracking of optimal reference trajectories [17] [18].

Regarding the first method, many researchers have been done in this field. In 1991, Taga demonstrated the effectiveness of this approach in unpredicted environments [1]. Since then, several attempts have been made to explore more the effectiveness of neural oscillator based controllers on legged locomotion [2]. However, sensory feedback signals also play a crucial role in such control systems. This technique has many advantages but also drawbacks that limit its utilization. The best advantage is its ability to learn through interaction with the environment. However, manual tuning of the oscillators parameters is required. In addition, many parameter optimization techniques were developed, but for the price of increased computational effort along with the increase of the state space dimension. This calculation time is too prohibitive and makes those techniques undesirable for implementation in real-time. Matsubara et al. [3] developed a new technique based on sensory feedback to CPG for adapting the controller to the environment, but also this technique has a high computational cost. So they went into a reduction of the state space dimensionality.

The second approach known as Passive dynamic walking pioneered by McGreer more than a decade ago [7] has been well studied by several researchers [4]-[6]. Passive dynamic walking is attractive for its elegance and simplicity, active feedback control is necessary to achieve walking on level ground and varying slopes, robustness to uncertainties and disturbances, and to regulate walking speed. The first result in active feedback control that exploits passive walking appeared in [5], [9], [10], [11], for planar bipeds. Passive walking in three dimensions was studied in [12] and [13]. Later the results in [11] were extended to the general case of 3-D walking in [14]. An interesting and elegant extension of these ideas appears in [15] where geometric reduction methods are used to generate stable 3-D walking from 2-D gaits. Robustness issues were addressed in [16] using total energy as a storage function in the hybrid passivity framework.

The third approach proposed by Sabourin et al. [8], is based on a control strategy that allows the transition of velocities for the dynamic walk of an under actuated two-dimensional robot without using a reference trajectory and by simple succession of active and passive phases.

The fourth approach [17][18] is based on the analysis of the variations of angles, velocity, and acceleration of human locomotion and trying to reproduce them on robots. This method has many drawbacks. First, to mimic human the robot dimensions should be customized to the model. Secondly this method cannot give the robot the possibility to adapt itself to the surrounding environment (in a non-regular ground for instance.).

In this paper, we propose to mimic human motion. This work could be considered as an enhancement to the idea proposed by Sabourin et al., and an extension to the real world of anthropomorphic three-dimensional robots with foot. The low level control is a PID controller. However, the high level control will be an adaptive control algorithm based on the predefined points we summarized from human locomotion and deduced from tests done by different

H. Serhan is with LISV Laboratory-Versailles S[t] Quentin University-France (phone: 961-3-317992; email: hserhan@hotmail.com)

P. Hénaff is with LISV Laboratory-Versailles S[t] Quentin University-France (phone: +331.39.25.49.91;email:patrick.henaff@uvsq.fr)

C. Nasr is with the Lebanese University - Faculty of Engineering I - Lebanon (phone: 961-3-369245; email: chnasr@ieee.org)

F. B. Ouezdou is with LISV -Versailles S[t] Quentin University–France (phone: +331.39.25.49.50;email:fethi.benouezdou@uvsq.fr)

researchers in this field. The proposed technique is not based on following a predefined trajectory; this will give the robot the possibility to adapt itself to the surrounding environment.

This paper is organized as follows: In section II, a description of the control technique is discussed in details along with a description of the robot and the simulator used. In section III, Implementation of the control algorithm and the results obtained will be presented in detail. Section IV concerns discussion and conclusion.

II. Control Method Description

A. The ROBIAN project

Our main motivation for bipedal research concerns a significant contribution to the study of human being locomotion system. For this purpose, a multi-degree of freedom biped prototype with flexible feet called ROBIAN (acronym for Robot BIpède ANthropomorphique), has been developed. The major application of ROBIAN (Fig. 1) prototype is the development of a real test bed of active/passive prosthesis devices enhancing research on the human being locomotion apparatus. ROBIAN is composed of two different parts: a locomotion system (lower limbs) and a torso mechanism (upper part). In this paper, we focus only on the locomotion systems. Each leg has a total of seven DoFs [17], [18], three actuated DoFs for the hip, one actuated for the knee, two actuated for the ankle and one passive for the foot providing flexible feet. The total height of robot is 1.50 m, its weight is 30 kg, and modular design was developed. Hence, each concerned kinematical module (hip, knee, ankle or foot) can be easily replaced by a prosthetic device to be tested. Mechanical construction of the modular locomotion system has already been done and static walking gaits were already achieved in 2003.

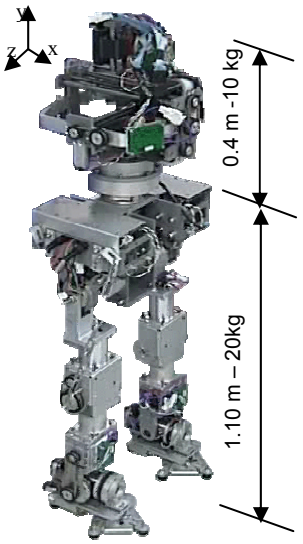

Fig. 1. The ROBIAN biped

B. Human motion & inspired walking parameters

The work on human locomotion done by, Viel [21], Bouisset [22], Allard [23], and Winter [24] allows us to identify the major properties in the human walking that influence step length, velocity, and equilibrium in a dynamic walk. The full human walking cycle described in [21], [22], [23], and [24], can be divided into eight phases. The functionality of each phase can be depicted with respect to one leg acting first as swing leg and then as stance leg (Fig. 2). Our description will be more physical in order to inspire the way the robot will be controlled.

Human locomotion is a succession of passive and active phases [8]. The locomotion of our anthropomorphic robot ROBIAN can be characterized by essential angles inspired from movements of the locomotion apparatus of human being in 3 plans (sagital "S", frontal "F" and transversal "T") [25],[26]. These angles could be summarized as follows (Fig. 3).

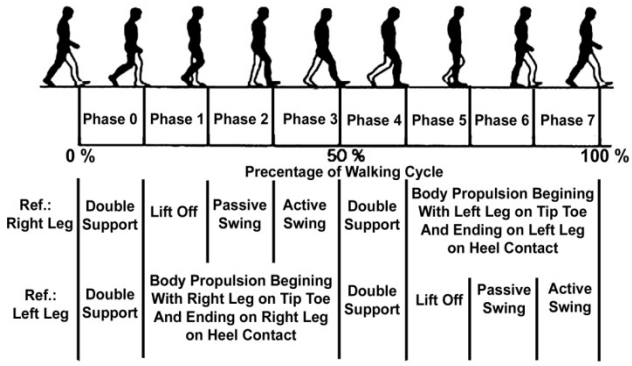

Fig. 2. Full Human Walking Cycle Description (Ref. Right Leg)

In Sagital plan (S plan):

Two angles that have direct effect on step length, and walk stability are:

- Swing leg Hip Anterior Extreme Angle: $\theta_{Max\_H\_S}^{SW}$
- Stance leg Hip Posterior Extreme Angle: $\theta_{Max\_H\_S}^{ST}$

Four angles that have direct effect on robot dynamics and propulsion are:

- Swing leg Knee Anterior Extreme Angle : $\theta_{Min\_K\_S}^{SW}$
- Swing leg Knee Posterior Extreme Angle: $\theta_{Max\_K\_S}^{SW}$
- Stance leg Knee Anterior Extreme Angle: $\theta_{Max\_K\_S}^{ST}$
- Swing leg Ankle Anterior Extreme Angle: $\theta_{Max\_A\_S}^{SW}$
- Upper Body Inclination Angle: $\theta_{Max\_S}^{UB}$ has direct effect on robot speed and stability. This is due to its effect on the position of the robot center of mass (section III.B.).

Based on the swing leg Tibia Ground Contact Angle $\theta_{GC\_S}^{SW}$, the control unit should regulate the lift off phase of the upcoming swing leg.

In Frontal Plan (F plan):

Two angles have direct effect on robot stability:

- Maximum Hip ABduction Angle: $\theta_{Max\_H\_F}^{DS}$
- Maximum Hip ADduction Angle: $-\theta_{Max\_H\_F}^{DS}$

In Transversal Plan (T plan):

In this plan, we are not taking into account hip movement because internal rotation movement of the human leg is negligible. We assume that the leg is not doing any rotation.

C. PD Controllers parameters

It should be noticed that all the motors are drove by PD controllers with the predefined angles (detailed in the paragraph B) as desired angles. A general equation of each PD controller of each actuator τ is given below:

$$\tau_{actuator\_plan}^{leg} = Kc_{actuator\_plan}^{phase} * (\theta_d - \theta) + Kd_{actuator\_plan}^{phase} * (\dot{\theta}_d - \dot{\theta}) \quad (1)$$

Where: θ and $\dot{\theta}$ are the relative angle & velocity of the corresponding actuator. θ_d and $\dot{\theta}_d$ are the desired angle and

velocity values. And *leg* corresponds to Stance or Swing leg, *phase* corresponds to phases from 0 to 7, *actuator* corresponds to Hip, Knee and Ankle, *plan* corresponds to Sagital, Frontal, and Transversal. At each phase, the values of the Kc, Kd parameters are changed. An empirical way was used for adjusting those parameters when the swing leg is near to touch the ground.

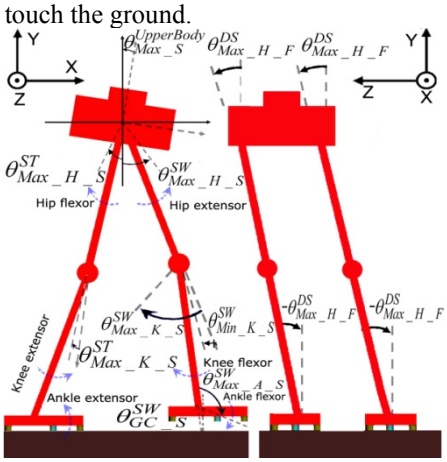

Fig. 3. Extreme angles characterizing ROBIAN Locomotion

D. *Inspired Control strategy*

Our control strategy consists in analyzing ROBIAN dynamic walk through the previously determined parameters (II.B.). We have divided our control algorithm into 12 states. States 1,3,4,5,6,10 correspond to the swing leg and states 2,7,8,9,11 correspond to the stance leg. They will actually happen in the same time if right & left leg motion during a half walking cycle is studied. The initial position is defined when the robot is standing up but one of the legs is behind the other. The control algorithm is defined by the below Petri Net Algorithm (Fig. 4). The control techniques along with the correspondence between the Petri Net Algorithm states and the human walking phases are given below:

State 0: Equilibrium Phase - where the robot is standing up with Stance Leg in front of Swing Leg. This state is the starting position.

State 1: (DS – F Plan) Move Weight to Stance Leg, this state corresponds to Human "Phase 0 - DS". This state is active only at startup. During this State, two actions happen in parallel:

- Apply an active torque to the Hip for moving body toward Stance Leg:

$$\tau^{SW}_{H\_F} = Kc^{0}_{H\_F} * (\theta^{DS}_{Max\_H\_F} - \theta^{SW}_{H\_F}) + Kd^{0}_{H\_F} * (\dot{\theta}^{DS}_{Max\_H\_F} - \dot{\theta}^{SW}_{H\_S})$$

- Activate Ankle in order to follow the inverse of the current Hip angle, this will lead to maintaining body parallel to ground:

$$\tau^{SW}_{A\_F} = Kc^{0}_{A\_F} * (-\theta^{SW}_{H\_F} - \theta^{SW}_{A\_F}) + Kd^{0}_{A\_F} * (-\dot{\theta}^{SW}_{H\_F} - \dot{\theta}^{SW}_{A\_F})$$

State 2: (DS – F Plan) Move Weight to Stance Leg, this state corresponds to Human "Phase 4 – DS". This state is active only at startup. During this State, two actions happen in parallel:

- Apply an active torque to the Hip for moving body toward Stance Leg:

$$\tau^{ST}_{H\_F} = Kc^{4}_{H\_F} * (\theta^{DS}_{Max\_H\_F} - \theta^{ST}_{H\_F}) + Kd^{4}_{H\_F} * (\dot{\theta}^{DS}_{Max\_H\_F} - \dot{\theta}^{ST}_{H\_S})$$

- Activate Ankle in order to follow the inverse of the current Hip angle:

$$\tau^{ST}_{A\_F} = Kc^{4}_{A\_F} * (-\theta^{ST}_{H\_F} - \theta^{ST}_{A\_F}) + Kd^{4}_{A\_F} * (-\dot{\theta}^{ST}_{H\_F} - \dot{\theta}^{ST}_{A\_F})$$

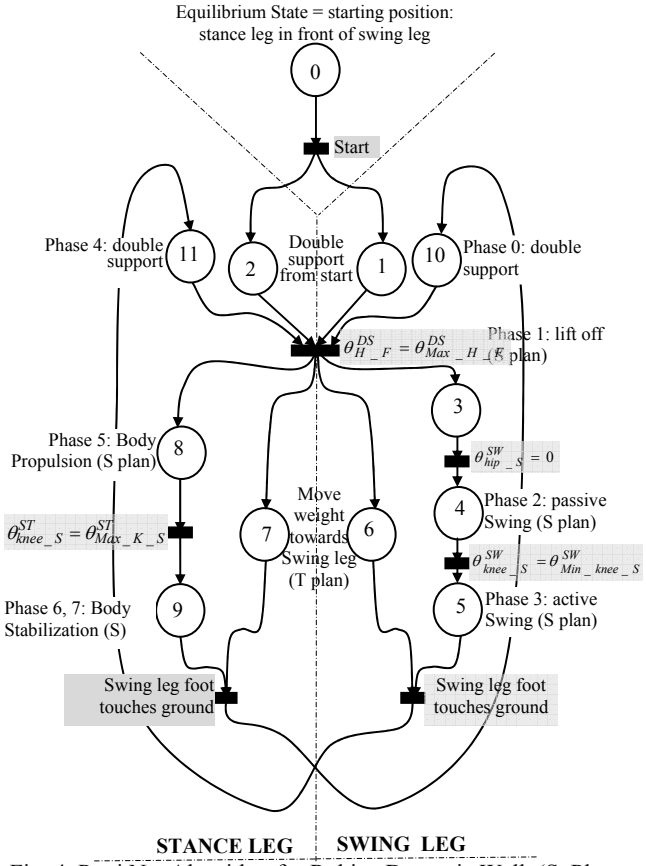

Fig. 4. Petri Net Algorithm for Robian Dynamic Walk (S_Plan or Sagital Plan, F_Plan or Frontal Plan)

State 3: (Swing Leg - S Plan) this State Corresponds to Human "Phase 1 – Liftoff". It starts after the hip angle in "T-plan" is equal to desired one, which indicates that most Body weight is applied on Stance leg. During this State, three actions happen in parallel:

- Apply an active torque to the Hip for accelerating the dynamic move of the oscillatory leg and create body inertial effects until thigh is in vertical position:

$$\tau^{SW}_{H\_S} = Kc^{1}_{H\_S} * (\theta^{SW}_{H\_S\_d} - \theta^{SW}_{H\_S})$$

- Keep Knee Free from any torque. It will bend in the opposite direction: $\tau^{SW}_{K\_S} = 0$
- Keep Ankle Free from any torque. This will extend ankle: $\tau^{SW}_{A\_S} = 0$

State 4: (Swing Leg – S Plan) this State Corresponds to Human "Phase 2 - Passive Swing". It starts when the Swing leg thigh is in vertical position. After this position, body will move forward under gravity. During this State, three actions happen in parallel:

- Keep Hip Free from any torque. Swing leg thigh inertia will impose its forward motion: $\tau^{SW}_{H\_S} = 0$

- Keep Knee Free from any torque. It will extend under gravity effects: $\tau^{SW}_{K\_S} = 0$
- Activate Ankle till Foot is parallel to Ground: $\tau^{SW}_{A\_S} = Kc^{2}_{A\_S} * (\theta^{SW}_{A\_S\_d} - \theta^{SW}_{A\_S}) + Kd^{2}_{A\_S} * (\dot{\theta}^{SW}_{A\_S\_d} - \dot{\theta}^{SW}_{A\_S})$

State 5: (Swing Leg – S Plan) this State Corresponds to Human "Phase 3 - Active Swing". This is the Swing leg landing phase. It starts when thigh of Swing leg reaches the posterior extreme angle. During this State, three actions happen in parallel:

- Apply an active torque to the Hip, for stabilizing it: $\tau^{SW}_{H\_S} = Kc^{3}_{H\_S} * (\theta^{SW}_{Max\_H\_S} - \theta^{SW}_{H\_S}) + Kd^{3}_{H\_S} * (\dot{\theta}^{SW}_{Max\_H\_S} - \dot{\theta}^{SW}_{H\_S})$
- Apply an active torque to the Knee, for stabilizing it: $\tau^{SW}_{K\_S} = Kc^{3}_{K\_S} * (\theta^{SW}_{Min\_K\_S} - \theta^{SW}_{K\_S}) + Kd^{3}_{K\_S} * (\dot{\theta}^{SW}_{Min\_K\_S} - \dot{\theta}^{SW}_{K\_S})$
- Apply an active torque to the Ankle for keeping Foot parallel to Ground: $\tau^{SW}_{A\_S} = Kc^{3}_{A\_S} * (\theta^{SW}_{Max\_A\_S} - \theta^{SW}_{A\_S}) + Kd^{3}_{A\_S} * (\dot{\theta}^{SW}_{Max\_A\_S} - \dot{\theta}^{SW}_{A\_S})$

State 6: (Swing Leg – F Plan) Move Weight smoothly toward Swing Leg, so body weight will be applied on swing leg when touching the ground. During this State, two actions happen in parallel:

- Apply an active torque to the Hip for moving body toward Swing Leg: $\tau^{SW}_{H\_F} = Kc^{0-4}_{H\_F} * (\theta^{ref}_{H\_F} - \theta^{SW}_{H\_F}) + Kd^{0-4}_{H\_F} * (\dot{\theta}^{ref}_{H\_F} - \dot{\theta}^{SW}_{H\_F})$

  With : $\theta^{ref}_{H\_F} = -\theta^{SW}_{H\_S} * \frac{\theta^{DS}_{Max\_H\_F}}{\theta^{SW}_{Max\_H\_S}}$
- Activate Knee in order to follow the inverse of the current Hip angle: $\tau^{SW}_{A\_F} = Kc^{0-4}_{A\_F} * (-\theta^{ref}_{H\_F} - \theta^{SW}_{A\_F}) + Kd^{0-4}_{A\_F} * (\dot{\theta}^{ref}_{H\_F} - \dot{\theta}^{SW}_{A\_F})$

State 7: (Stance Leg – F Plan) Move Weight toward Swing Leg. During this State, two actions happen in parallel:

- Apply an active torque to the Hip for moving body toward Stance Leg: $\tau^{ST}_{H\_F} = Kc^{0-4}_{H\_F} * (\theta^{ref}_{H\_F} - \theta^{ST}_{H\_F}) + Kd^{0-4}_{H\_F} * (\dot{\theta}^{ref}_{H\_F} - \dot{\theta}^{ST}_{H\_F})$

  With : $\theta^{ref}_{H\_F} = -\theta^{SW}_{H\_S} * \frac{\theta^{DS}_{Max\_H\_F}}{\theta^{SW}_{Max\_H\_S}}$
- Activate Knee in order to follow the inverse of the current Hip angle: $\tau^{ST}_{A\_F} = Kc^{0-4}_{A\_F} * (-\theta^{ref}_{H\_F} - \theta^{ST}_{A\_F}) + Kd^{0-4}_{A\_F} * (\dot{\theta}^{ref}_{H\_F} - \dot{\theta}^{ST}_{A\_F})$

State 8: (Stance Leg - S Plan) this State Corresponds to Human "Phase 5 - Body Propulsion". During this State, three actions happen in parallel:

- Apply an active torque to the Hip for stabilizing Upper Body and counteracting swing leg hip torque: $\tau^{ST}_{H\_S} = Kc^{5}_{H\_S} * (\theta^{UB}_{Max\_S} - \theta^{ST}_{H\_S}) + Kd^{5}_{H\_S} * (\dot{\theta}^{UB}_{Max\_S} - \dot{\theta}^{ST}_{H\_S})$
- Apply an active torque to the Knee for extending it and initiate body propulsion: $\tau^{ST}_{K\_S} = Kc^{5}_{K\_S} * (\theta^{ST}_{Max\_K\_S} - \theta^{ST}_{K\_S}) + Kd^{5}_{K\_S} * (\dot{\theta}^{ST}_{Max\_K\_S} - \dot{\theta}^{ST}_{K\_S})$
- Keep Ankle Free from any torque (this is an essential action for freeing body propulsion): $\tau^{ST}_{A\_S} = 0$

State 09: (Stance Leg – S Plan) this state corresponds to Human "Phase 6, 7 - Body Stabilization". It starts when Stance leg knee angle is extended and reaches $\theta^{ST}_{Max\_K\_S}$. During this State, three actions happen in parallel:

- Stabilize Upper Body: $\tau^{ST}_{H\_S} = Kc^{6}_{H\_S} * (\theta^{UB}_{Max\_S} - \theta^{ST}_{H\_S}) + Kd^{6}_{H\_S} * (\dot{\theta}^{UB}_{Max\_S} - \dot{\theta}^{ST}_{H\_S})$
- Stabilize Knee: $\tau^{ST}_{K\_S} = Kc^{6}_{K\_S} * (\theta^{ST}_{Max\_K\_S} - \theta^{ST}_{K\_S}) + Kd^{6}_{K\_S} * (\dot{\theta}^{ST}_{Max\_K\_S} - \dot{\theta}^{ST}_{K\_S})$
- Keep Ankle Free from any torque (this is essential for freeing body propulsion): $\tau^{ST}_{A\_S} = 0$

State 10: (DS – F Plan) Move Weight to Stance Leg, this state corresponds to Human "Phase 0 - DS". During this State, two actions happen in parallel:

- Apply an active torque to the Hip for moving body toward Stance Leg: $\tau^{SW}_{H\_F} = Kc^{0}_{H\_F} * (\theta^{DS}_{Max\_H\_F} - \theta^{SW}_{H\_F}) + Kd^{0}_{H\_F} * (\dot{\theta}^{DS}_{Max\_H\_F} - \dot{\theta}^{SW}_{H\_S})$
- Activate Knee in order to follow the inverse of the current Hip angle: $\tau^{SW}_{A\_F} = Kc^{0}_{A\_F} * (-\theta^{SW}_{H\_F} - \theta^{SW}_{A\_F}) + Kd^{0}_{A\_F} * (-\dot{\theta}^{SW}_{H\_F} - \dot{\theta}^{SW}_{A\_F})$

State 11: (DS – F Plan) Move Weight to Stance Leg, this state corresponds to Human "Phase 4 - DS". During this State, two actions happen in parallel:

- Apply an active torque to the Hip for moving body toward Stance Leg: $\tau^{ST}_{H\_F} = Kc^{4}_{H\_F} * (\theta^{DS}_{Max\_H\_F} - \theta^{ST}_{H\_F}) + Kd^{4}_{H\_F} * (\dot{\theta}^{DS}_{Max\_H\_F} - \dot{\theta}^{ST}_{H\_S})$
- Activate Knee in order to follow the inverse of the current Hip angle: $\tau^{ST}_{A\_F} = Kc^{4}_{A\_F} * (-\theta^{ST}_{H\_F} - \theta^{ST}_{A\_F}) + Kd^{4}_{A\_F} * (-\dot{\theta}^{ST}_{H\_F} - \dot{\theta}^{ST}_{A\_F})$

III. SIMULATION RESULTS

We applied this algorithm on a simulated model of our biped robot ROBIAN developed under OpenHRP (Open Architecture Humanoid Robotics Platform) the software platform for dynamic simulation of humanoid robots, developed by AIST, the University of Tokyo and MSTC This simulator allows us to evaluate the robustness of our approach before testing on the real robot. The OpenHRP model of the ground/foot contact is based on a spring-damper system. In our case, the parameters Kp (spring coefficient) and Cp (damper coefficient) are calculated experimentally.

- Spring-damper coefficients parallel to axis [X, Y, Z]:
$K_P = [10^5, 10^5, 10^5]$ *in N/m;* $C_P = [10^4, 10^4, 10^4]$ *in N/(m/sec);*
- Spring-damper coefficients rotational around axis [X,Y,Z]:
$K_R = [1.610^4, 10^3, 10^3]$ *in Nm/rad;*
$C_R = [1.610^3, 10^2, 10^2]$ *in Nm/(rad/sec);*

ROBIAN foot contains 5 similar plots in rubber. Below are

the Static and sliding friction factors:
Static friction factor = 0.6, sliding friction factor = 0.5.

A. Walking analysis

Walking snapshots from frontal and S plan are represented on Fig. 6 (walking speed is of 0.65 m/sec).

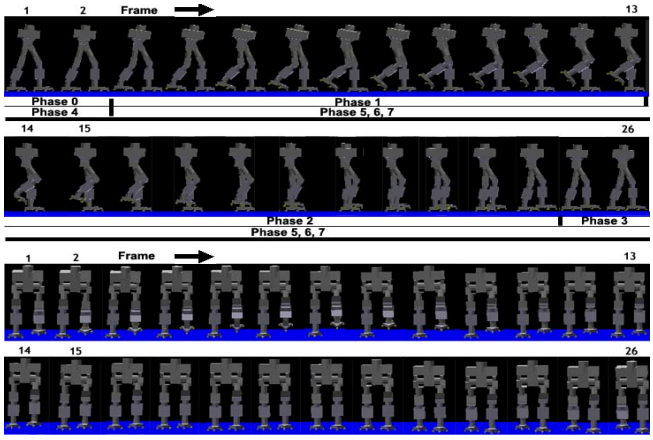

Fig. 6. Walking snapshots from F (up) and S plans (bottom) for a half walking cycle at the speed of 0.65m/s. Time between each snapshot is 19ms (frames captured from left to right).

The superposition of successive walking phases presented in Fig 10 shows the stability of a long walk of the robot (ie. ten walking cycles). The results obtained show that ROBIAN was able to walk infinitely into the simulator without falling. This is due to the continuous control of the PD controllers parameters based on the walking phases, thus based on the joint positions.

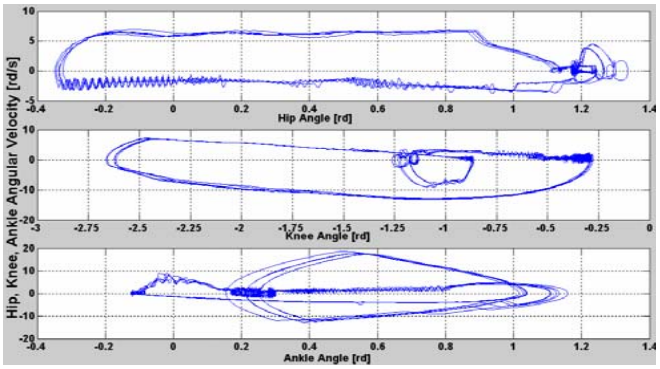

Fig. 10. Phase succession for ten walking cycles (angular velocity of Hip, Knee and ankle function of their corresponding angle

B. Control of the Robot speed and walk stability

Walking speed and stability is primary influenced by four parameters: $\theta^{UB}_{Max\_S}$ affects the robot center of mass position, $\theta^{SW}_{Max\_H\_S}$, $\theta^{S\tan ce}_{Max\_K\_S}$ and $\theta^{SW}_{Min\_knee\_xy}$ affect the step length and body propulsion velocity. So with a simple variation of those four reference angle values, the step length and hence the walking speeds of the robot are controlled. The duration of one complete walking cycle is about 1 sec. Fig. 7 shows the robot mean speed variation with respect to upper body inclination angle $\theta^{UB}_{Max\_S}$. We can deduce that increasing this latter one will contribute to higher walking speed. A limit for this angle (18 degrees) is determined. In Fig. 8, the robot mean speed variation with respect to angle $\theta^{SW}_{Min\_K\_S}$ is given. Hip anterior extreme angle $\theta^{SW}_{Max\_H\_S}$ has also some influence on robot walking speed.

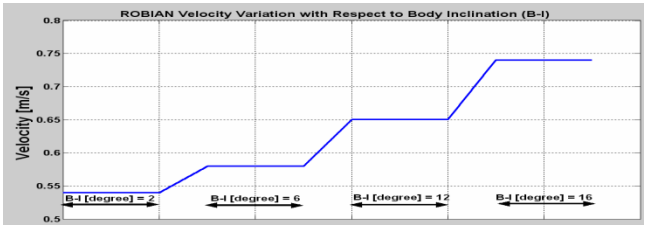

Fig. 7. ROBIAN means velocity value with respect to Body Inclination (knee anterior extreme angle is fixed to -4 degree)

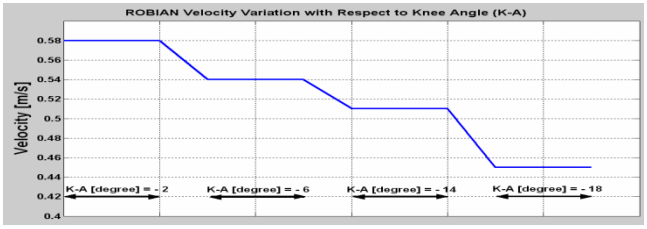

Fig.8. ROBIAN mean velocity value with respect to knee anterior extreme angle (body inclination is fixed to 6 degree)

After hundreds of tests, stability margin for different referenced angles is summarized in the Table II.

Table II
Stability Limit Margins

$\theta^{SW}_{Max\_H\_S}$		$\theta^{ST}_{Max\_H\_S}$		$\theta^{SW}_{Min\_K\_S}$	
Acceptable margin	*Currently allocated*	*Acceptable margin*	*Currently allocated*	*Acceptable margin*	*Currently allocated*
20° to 40°	***30°***	***-20° to -10°***	***-15°***	***-30° to -2°***	***-4°***
$\theta^{SW}_{Max\_K\_S}$		$\theta^{ST}_{Max\_K\_S}$		$\theta^{SW}_{Max\_A\_S}$	
Acceptable margin	*Currently allocated*	*Acceptable margin*	*Currently allocated*	*Acceptable margin*	*Currently allocated*
-85° to -55°	***-75°***	***0° to 50°***	***35°***	***0° to 50°***	***35°***
$\theta^{UB}_{Max\_S}$		$\theta^{DS}_{Max\_H\_F}$			
Acceptable margin	*Currently allocated*	*Acceptable margin*	*Currently allocated*		
0° to 18°	***6°***	***0° to 10°***	***4°***		

C. Power consumption analysis

In order to implement the control algorithm on the real robot ROBIAN, the technological limits of the actuators should be taken into account. The motors used are from Maxon manufacturer (the 90Watts RE35 is installed on the three hip and one knee joints and the 150Watts RE40 is installed on the two ankle ones). The power issued from those motors should be within the real limits. The value of the motor velocity reduction can be changed in order to ensure that the maximum velocity and maximum torque for each motor is under the values specified into the datasheet. Fig. 11 plots the graphs of the motors zone of functionality. All the motor specifications (velocity, torque and power) are taken into consideration. Those graphs were evaluated at the maximum walking speed of the robot in which case the motors are stressed the most. Taking into account our

walking gait, the values of the torques (12 Nm at the hip, 8 Nm at knee and ankle) are sufficient.

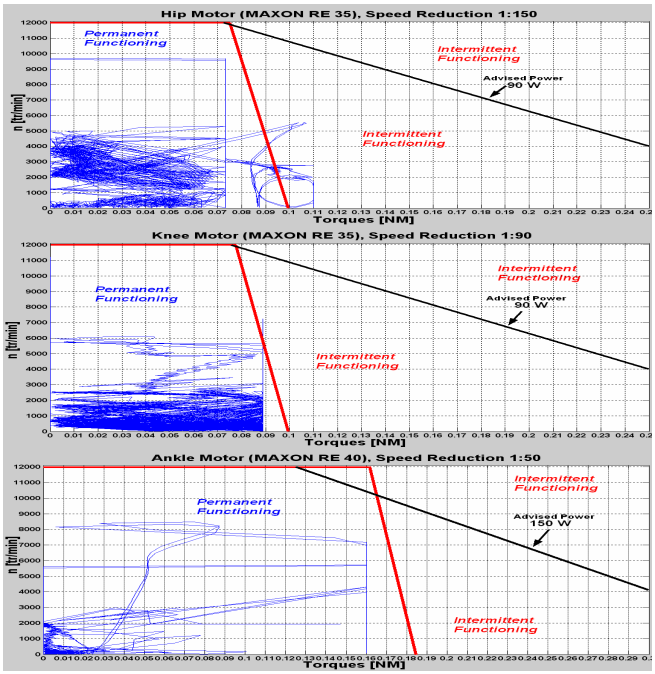

Fig. 11. Graphs of hip, knee, and ankle motors functionality under the motor physical limits for one complete walking cycle.

IV. Discussion and Conclusion

We achieved our goal in making in simulation the ROBIAN robot walk in 3D. We approached the human walking angles without a lot of complexity in the control. Also the feet land parallel to ground, the swinging leg will have the foot moving as human in the beginning of the swing phase. In passive swing phase, ankle motors were controlled in order to keep the foot parallel to ground. In the active swing phase, the foot was stabilized in this position in order to hit the ground in a way so that the ground reaction forces will be distributed equally on the five foot plots. In order to approach the smoothness of human neuromuscular commands, a muscle model created by Serhan et al. [28] is added to ROBIAN low level control stage. This model is based on a PID controller and a DC motor. Hence, it will be easily integrated into our control diagram without making any changes, neither to the underlying hardware system nor to the high level control algorithm. Also this technique is not very consuming in processing time (algorithm execution time is about 8ms on a Pentium IV processor running at 3.0 Ghz with 1 GB RAM), so it could be implemented easily in real-time. We are working now to validate our approach on the real biped ROBIAN. A next work will concern the control of transition between walking phase and stop phase. In conclusion, the proposed approach, allows us to achieve Robian dynamic walking similar to that of human.

References

[1] G. Taga, Y.Yamaguchi, H. Shimizu, "Self-organized control of bipedal locomotion by neural oscillators in unpredictable environment," Biological Cybernetics 65,1991 ,147-159

[2] G. Endo, J. Morimoto, J. Nakanishi, G. Cheng, "An empirical exploration of a neural oscillator for biped locomotion control," IEEE, Int. Conference on Robotics and Automation, 2004, pp. 3036-3042

[3] T. Matsubara, J. Morimoto, J. Nakanishi, M. Sato, K. Doya, "Learning CPG-based biped locomotion with a policy gradient method," Robotics and Autonomous Systems 54 ,2006, 911-920

[4] M.Garcia, A. Chatterjee, A. Ruina, and M. Coleman, "The simplest walking model: Stability, complexity, and scaling," ASME J. Biomechan. Eng., vol. 120, no.2, pp. 281-288, 1998.

[5] A. Goswami, B. Espiau, and A. Keramane, "Limit cycles in a passive compass gait and passivity-mimicking control laws," Autonomous Robots, vol. 4, no. 3, pp. 273-286, 1997.

[6] A. Goswami, B. Thuilot, and B. Espiau, "A study of the passive gait of a compass-like biped robot: Symmetry and chaos," I. J. Robot. Res., vol. 17, no. 12, pp. 1282-1301, 1998.

[7] T. McGreer, "Passive dynamic walking," Int. J. Robot, Res., vol. 9, no. 2, pp. 62-82, 1990.

[8] C. Sabourin, O. Bruneau, J-G. Fontaine. "Pragmatic rules for real-time control of the dynamic walking of an under-actuated biped robot," Proc. IEEE Conf. on Rob. and Automation, 2004, 4216–4221

[9] H. Ohta, M. Yamakita, and K. Furuta, " From Passive to active dynamic walking," in Proc. IEEE Conf. Decision Control, Phoenix, AZ, Dec.1999, pp.3883-3885.

[10] M.W. Spong, "Bipedal locomotion, robot gymnastics, and motor air hockey: A rapprochement," in Proc. TITech COE/Super Mechano-Systems workshop, Tokyo, Japan, Feb. 1999, pp. 34-41.

[11] M.W. Spong, "Passivity based control of the campass gait biped," in Proc. IFAC Trienmial World Congr., Beijing, China, vol. 3, July 1999, pp. 19-23.

[12] A.D. Kuo, "Stabilization of lateralmotion in passive dynamic walking," Int. J. Robot. Res., vol. 18, no. 9, pp. 917-930, 1999.

[13] S.H. Collins, M. Wisse, and A. Ruina, "A three-dimensional passive dynamic walking robot with two legs and knees," Int. J. Robot. Res., vol. 20, 4, no. 3, pp. 273-286, 1997.

[14] M.w. Spong and F. Bullo, "Controlled symmetrics and passive walking,"IEEE trans. Aut. Contr., vol. 50, no. 7, pp. 1025-1031, 2005.

[15] A.D. Ames, R.D. Gregg, E.D.B. Wendel, and S. Sastry, "Towards the geometric reduction of controlled three-dimensional robotic bipedal walkers," in Proc. Workshop Lagrangian Hamiltonian Methods Nonlinear Control, Nagoya, Japan, July 2006, pp. 117-124.

[16] M.W. Spong and G. Bhatia, "Further results on control pf the compass gait biped," in Proc. IROS 2003, Las Vegas, Nevada, 27-30 Oct.. 2003, pp. 1933-1938.

[17] A. Konno, R. Sellaouti, F.B. Amar, and F.B. Ouezdou. "Design and development of the biped prototype ROBIAN". In IEEE Int. Conf. on Rob. and Aut. (ICRA), D.C., U.S.A., 2002, pp. 1384–1389.

[18] R. Sellaouti and F. B. Ouezdou, Design and control of a 3DOFs parallel actuated mechanism for biped application, Mechanism and Machine Theory, Volume 40, N°12, pages 1367-1393, dec. 2005.

[19] C Chevallereau, Y Aoustin, Optimal reference trajectories for walking and running of a biped robot, Robotica **19** (2001), pp. 557–569.

[20] Z. Tang, Z. Sun, C. Zhou and L. Hu, "Reference Trajectory Generation for 3-Dimensional Walking of a Humanoid Robot" Tsinghua Science & Technology Volume 12, Issue 5, October 2007, Pages 577-584

[21] E.Viel, "La marche humaine, la course et le saut," Masson, 2000.

[22] S. Bouisset, B. Maton, "Muscles, posture et mouvement," Hermann, 1995

[23] P. Allard, J.-P. Blanchi., "Analyse du mouvement humain par la biomécanique," 2000, Décarie.

[24] D. Winter, "Biomechanics and Motor Control of Human Movement," Third Edition, Wiley 2005.

[25] Bouchet A., Cuilleret J., "Anatomie topographique, descriptive et fonctionnelle", T3b le membre inférieur. SIMEP 3rd ed. 1997

[26] Kapandji I., "Physiologie articulaire, tome Membre inférieur", Maloine, 5th edition, 1999

[27] C. Williams, "Tuning a PID Temperature Controller," http://newton.ex.ac.uk/teaching/CDHW/Feedback/Setup-PID.html.

[28] Serhan H., Nasr C., Henaff P., "Designing a Muscle Like System Based on PID Controller and Tuned by Neural Network",IEEE WCCI Congress, Vancouver, 2006,pp. 10090-10097